# SUBSONIC AND TRANSONIC FLOW SIMULATION FOR A WING OSCILLATING IN YAW AND SIDESLIP

Koji Isogai Japan Aerospace Exploration Agency

**Keywords**: yaw, sideslip, transonic flow, CFD

# **Abstract**

As is well known, the flutter speed of T-tail depends strongly on the steady lift or dihedral angle of the horizontal tail plane. The unsteady rolling moment acting on the horizontal tail plane oscillating in yaw and sideslip plays the critical roll for this phenomenon. In this paper, a numerical method based on the 3D Navier-Stokes equations for computing the subsonic and transonic flow for a wing oscillating in yaw and sideslip is presented. By introducing a new coordinate system oscillating in yaw and sideslip, the existing 3D Navier-Stokes code is easily modified to account for the in-plane motions. The calculated rolling moments show a good agreement with the existing experimental data obtained for incompressible flow, and the effect of compressibility, especially the effects of the shock wave in transonic flow on the rolling moment are clarified.

#### 1 Introduction

It has been pointed out that flutter speed of Ttail depends strongly on the angle of attack and dihedral angle of the horizontal tail plane (HTP). This phenomenon was first recognized in the investigation processes of the accident of Handley Page "Victor" in 1954 [1]. The mechanism of the phenomenon can be explained by the fact that the rolling moment produced by the yawing and sideslip oscillation of HTP, which is induced by the torsional and bending oscillation of the vertical tail plane (VTP), depends on the angle of attack and dihedral angle of HTP. This mechanism has been clearly shown in flutter analyses of the several T-tail configurations by Wshizu et al. [2] and Jennings and Berry [3] and van Zyl and

Mathews [4]. Washizu et al. [2] and Jennings and Berry [3] used the quasi-steady strip aerodynamic forces to evaluate the rolling moments due to in-plane motions of HTP. Van Zyl and Mathews [4] extended the conventional Doublet Lattice Method to account for these aerodynamic loads using the lifting-line concept proposed by Queijo [5]. The exact liftingsurface theory for a wing oscillating in yaw and sideslip was developed by Isogai and Ichikawa [6] in 1973. Isogai [7] also extended their theory to T-tail configuration, which takes into account the in-plane motion of HTP. Unfortunately however, their theory can be applied only to incompressible flow, though the effect of compressibility, especially in transonic flow, on the T-tail flutter is important. Ruhlin et al. [8] conducted experimental studies of transonic Ttail flutter of a wide-body cargo/transport airplane. They found that the transonic antisymmetric flutter boundary for this T-tail showed an unusual sharp dip between a Mach number of 0.92 and 0.98.

Recently, the computational fluid dynamics has been applied to transonic flutter of T-tail configurations. Arizono et al. [9] presented the numerical simulation of a T-tail configuration using an Euler code. The flutter predicted was a symmetrical flutter for which the effect of inplane motion of HTP is not important. Therefore, the capability of the method for predicting the effects of the in-plane motion of HTP has not been clarified. Attorni, et al. [10] have also conducted the T-tail flutter simulation of P180 aircraft using an Euler code. However, the accuracy of the method has not been confirmed because no comparison with the experimental data was made.

The purpose of the present study is to present the numerical method for predicting the rolling moment acting on a wing oscillating in yaw and sideslip in subsonic and transonic flow as a first step to T-tail configuration.

### 2 Numerical Method

In order to conduct the numerical simulation for a wing oscillating in yaw and sideslip, we introduce the new coordinate system which is fixed on the wing oscillating in yaw and sideslip. Figure 1 shows the definition of the coordinate systems. The *xyz* coordinate system is fixed to the free-stream and the *x'y'z'* coordinate system is fixed on the wing oscillating in yaw and sideslip. The relation between the two coordinate systems can be given by

$$x = x' + \Psi z'$$
,  $y = y'$ ,  $z = z' + H - \Psi(x' + a)$  (1)

where  $\Psi$  and H are the yawing and sideslip displacements, respectively and a is the axis of yaw (positive toward the leading edge). (Note that length is made non-dimension by root semichord length b.) In Eq. (1), the higher order terms of  $\Psi$  and H are neglected. The conventional 3D Navier-Stokes (NS) code can be modified easily by changing the metric terms [11] such as  $\xi_x$ ,  $\xi_y$ ,  $\xi_z$ , etc. which transform the 3D NS equations in the xyz coordinate system into the computational space ( $\xi$ ,  $\eta$ ,  $\zeta$ ), namely,

$$\begin{split} \xi_{x} &= J(y'_{\eta} \left( -\Psi x'_{\zeta} + z'_{\zeta} \right) - y'_{\zeta} \left( -\Psi x'_{\eta} + z'_{\eta} \right) \right) \\ \xi_{y} &= J(z'_{\eta} x'_{\zeta} - x'_{\eta} z'_{\zeta} \right) \\ \xi_{z} &= J(y'_{\zeta} \left( \Psi z'_{\eta} + x'_{\eta} \right) - y'_{\eta} \left( \Psi z'_{\zeta} + x'_{\zeta} \right) \right) \\ \eta_{x} &= J(y'_{\zeta} \left( -\Psi x'_{\xi} + z'_{\xi} \right) - y'_{\xi} \left( -\Psi x'_{\zeta} + z'_{\zeta} \right) \right) \\ \eta_{y} &= J(x'_{\xi} z'_{\zeta} - x'_{\zeta} z'_{\xi} \right) \\ \eta_{z} &= J(y'_{\xi} \left( \Psi z'_{\zeta} + x'_{\zeta} \right) - y'_{\zeta} \left( \Psi z'_{\xi} + x'_{\xi} \right) \right) \\ \zeta_{x} &= J(y'_{\xi} \left( -\Psi x'_{\eta} + z'_{\eta} \right) - y'_{\eta} \left( -\Psi x'_{\xi} + z'_{\xi} \right) \right) \\ \zeta_{y} &= J(x'_{\eta} z'_{\xi} - x'_{\xi} z'_{\eta} \right) \\ \zeta_{z} &= J(y'_{\eta} \left( \Psi z'_{\xi} + x'_{\xi} \right) - y'_{\xi} \left( \Psi z'_{\eta} + x'_{\eta} \right) \right) \\ \xi_{t} &= - (d\Psi / dt) z'_{\xi} \zeta_{x} - y'_{t} \zeta_{y} - (dH / dt - d\Psi / dt(x' + a)) \xi_{z} \\ \eta_{t} &= - (d\Psi / dt) z'_{\eta} \gamma_{x} - y'_{t} \eta_{y} - (dH / dt - d\Psi / dt(x' + a)) \eta_{z} \end{split}$$

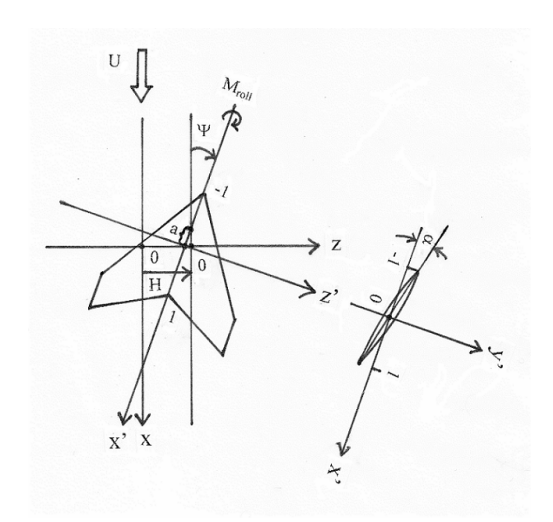


Fig. 1. Definition of Coordinate Systems.

$$\zeta_t = -(d\Psi/dt)z'\zeta_x - y'_t\zeta_y - (dH/dt - d\Psi/dt(x'+a))\zeta_z$$
(2)

Where J is the Jacobian of the transformation metrics and is given by

$$J^{-1} = x'_{\xi} y'_{\eta} z'_{\zeta} + x'_{\zeta} y'_{\xi} z'_{\eta} + x'_{\eta} y'_{\zeta} z'_{\xi} - x'_{\xi} y'_{\zeta} z'_{\eta} - x'_{\eta} y'_{\xi} z'_{\zeta} - x'_{\zeta} y'_{\eta} z'_{\xi}$$
(3)

Note that no special treatment in the conventional NS code such as the far-field boundary conditions and the surface boundary conditions in the new x'y'z' coordinate system once we replace the conventional metrics with those given by Eqs. (2).

The 3D NS code used in the present study is a Reynolds Averaged Navier-Stokes (RANS) code originally developed by Isogai [12]. A body-fitted C-H type grid is used. The number of grid points used is 240 points (200 points on the wing and 20 points on the upper and lower surfaces of the wake region) in the chord-wise direction, 58 points in the span-wise direction (38 points on the full span wing and 20 points on the off-wing region) and 51 points normal to the wing surface. The code employs a total variation diminishing (TVD) scheme [13] and the Baldwin and Lomax [14] algebraic turbulence model.

# 3 Results and Discussion

# 3.1 Incompressible Flow

In order to validate the present method, the numerical simulation of the flow for a wing oscillating in vaw, for which the experimental data [15] of rolling moment are available for incompressible flow, has been conducted. The first case is a rectangular wing of aspect-ratio 3. The chord and span of the wing are 0.20 m and 0.60 m, respectively, and it has the wing section of NACA0012. The angle of attack ( $\alpha$ ) and the dihedral angle (I) are 5.58 deg and 10 deg, respectively. amplitude The oscillation ( $\Psi_a$ ) is 6 deg and the axis of yaw (a) is at the mid-chord. The yawing displacement is given by

$$\Psi = \Psi_{o} \sin \omega t \text{ or } \Psi = \Psi_{o} \sin kt^*$$
 (4)

where t is time and  $\omega$  is circular frequency of oscillation, k is the reduced frequency defined by  $k=b\omega/U$  (U: free-stream velocity) and  $t^*$  is the dimensionless time defined by  $t^*=tU/b$ . For this wing the experimental [15] and theoretical results obtained by the lifting-surface theory [6] are available. The numerical simulation using the present 3D NS code has been conducted at  $M_{\infty}=0.30$  for this incompressible flow case. Figure 2 shows the variations of the amplitude and phase angle of rolling moment, which are obtained by the experiment [15], the lifting-surface theory [6] and the present numerical simulation. In the figure, the rolling moment coefficient ( $C_r$ ) is defined by

$$C_r = M_r / (4\rho U^2 b l^2 \Psi_o) \tag{5}$$

where  $M_r$  is the rolling moment (positive right wing down),  $\rho$  is far-field air density and l is semi-span. And  $\phi$  is the phase advance angle ahead of the yawing displacement. The results obtained by the present numerical simulation show a good agreement with those obtained by the experiment and the lifting-surface theory. In Fig. 3, the variations of rolling moment computed by the present 3D NS code and the yawing displacement during one cycle of oscillation are shown for k=0.30 and 0.50. Figure 4 shows the upper surface pressure

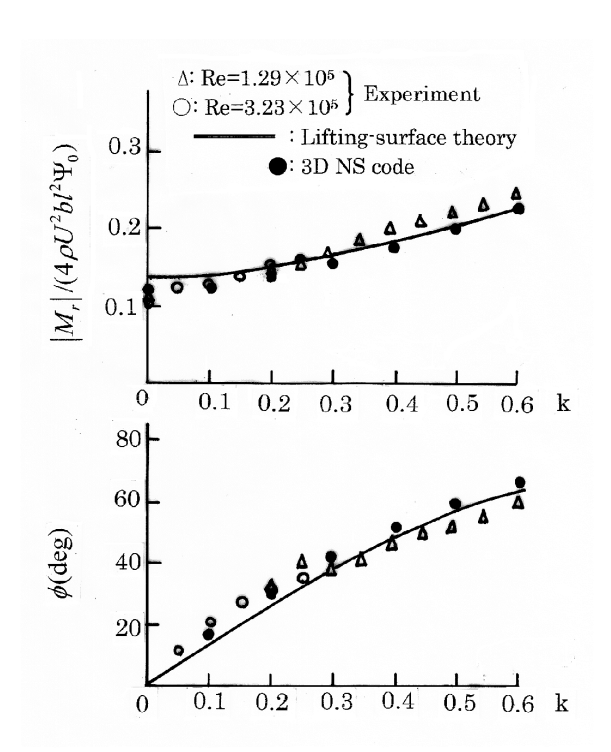


Fig. 2. Variations of Magnitude and Phase Angle of Rolling Moment with respect to Reduce Frequency (Rectangular Wing,  $\alpha$ =5.58 deg and  $\Gamma$ =10 deg).

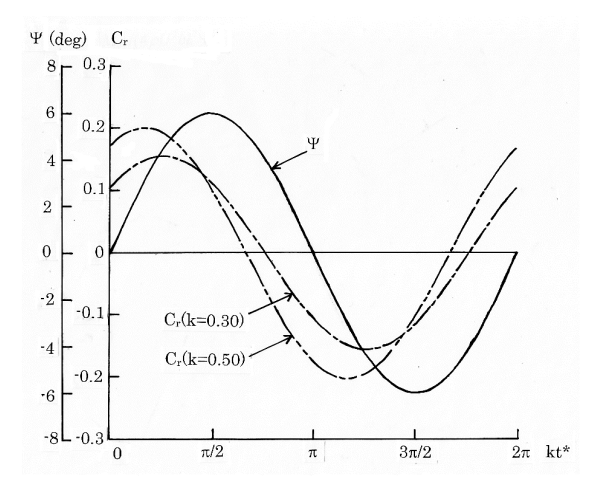


Fig. 3. Variations of Rolling Moment and Yawing Displacement for Rectangular Wing  $(M_{\infty}=0.30, \alpha=5.58 \text{ deg}, \Gamma=10 \text{ deg}, \Psi=6^{\circ}\text{sinkt*}).$ 

distributions at the typical phases of the oscillation at  $M_{\infty}$ =0.30 and k=0.50.

The second case is a sweptback wing of aspect-ratio 3 oscillating in yaw. The taper-ratio and swept angle are 1.0 and 30 deg, respectively. The chord length and span are 0.20 m and 0.60 m, respectively. For this wing, the experimental

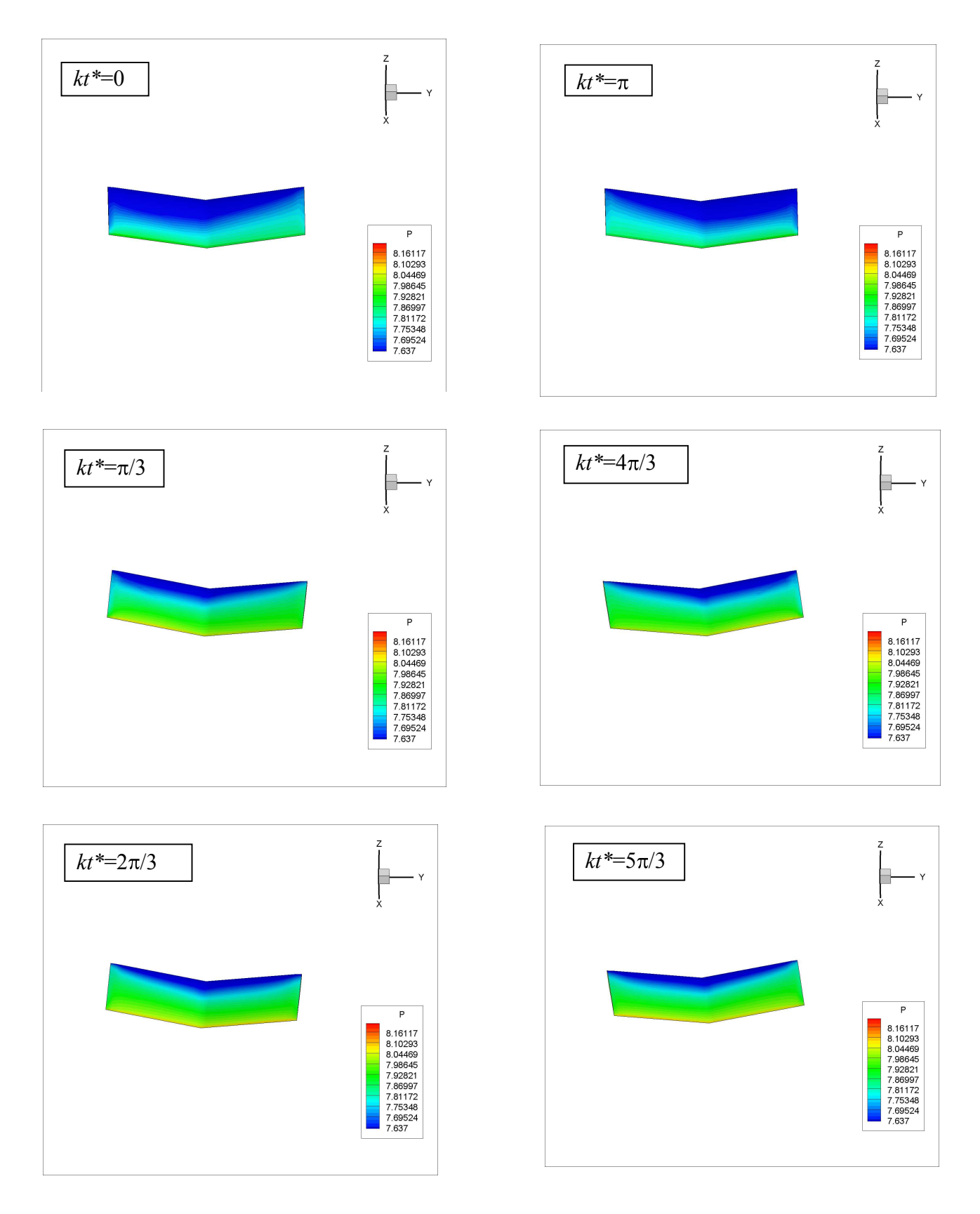


Fig. 4. Upper Surface Pressure Distributions during One Cycle of Oscillation (Rectangular Wing,  $M_{\infty}$ =0.30, k=0.50,  $\alpha$ =5.58 deg,  $\Gamma$ =10 deg,  $\Psi$ =6°sinkt\*).

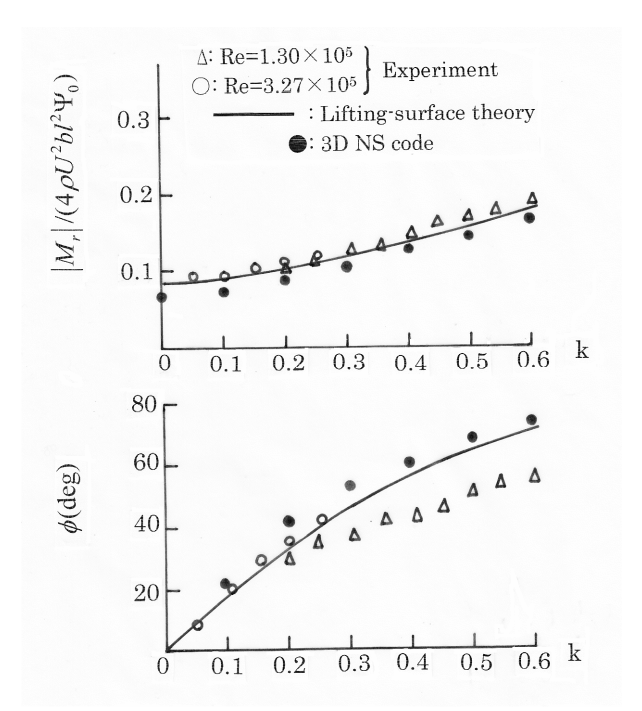


Fig. 5. Variations of Magnitude and Phase Angle with respect to Reduced Frequency (Sweptback Wing,  $\alpha$ =5.2 deg and  $\Gamma$ =0 deg).

data [15] of the rolling moment together with those obtained by the lifting-surface theory [6] are also available. The angle of attack and the dihedral angle are 5.2 deg and 0 deg, respectively. Figure 5 shows the variations of the amplitude and phase angle of the rolling moment with respect to the reduced frequency which are obtained by the experiment [15], the lifting-surface theory [6] and the present numerical simulation. The results of the present simulation show a satisfactory agreement with those of the lifting-surface theory and the experimental data. Figure 6 shows the variations of the rolling moment computed by the present 3D NS code and the yawing displacement during one cycle of oscillation for k=0.30 and 0.50.

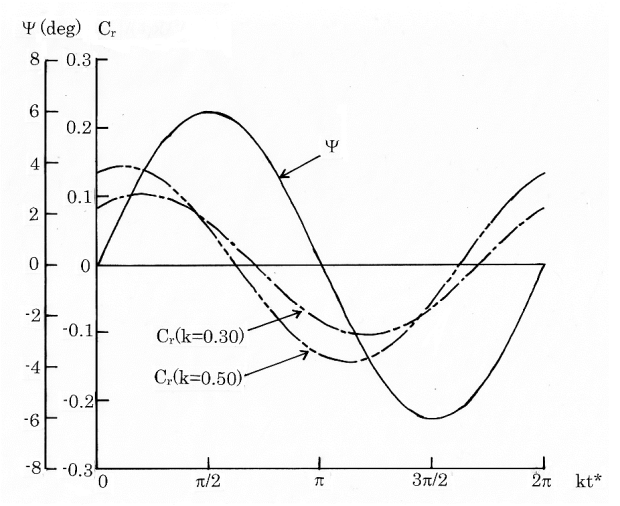


Fig. 6. Variations of Rolling Moment and Yawing Displacement for Sweptback Wing  $(M_{\infty}=0.30, \alpha=5.2 \text{ deg}, \Gamma=0 \text{ deg}, \Psi=6^{\circ} \text{sinkt*}).$ 

# 3.2 Effect of Compressibility

In order to see the effect of compressibility, the rolling moment (magnitude and phase angle) for  $M_{\infty}$ =0.30~0.75 for the same rectangular wing

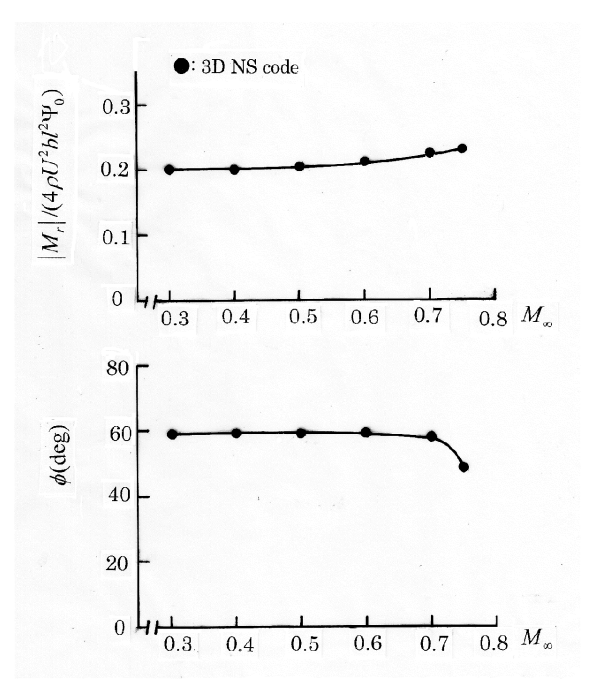


Fig. 7. Effect of Mach Number on Magnitude and Phase Angle of Rolling Moment for Rectangular Wing Oscillating in Yaw (k=0.50,  $\mathcal{Y}_o$ =6 deg).

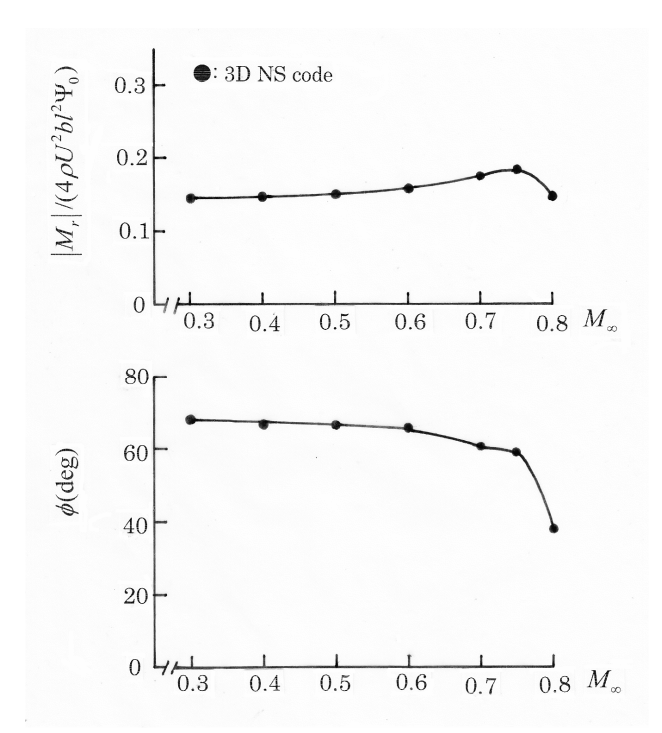


Fig. 8. Effect of Mach Number on Magnitude and Phase Angle of Rolling Moment for Sweptback Wing Oscillating in Yaw (k=0.50,  $\Psi_o$ =6 deg).

(as used for the incompressible flow case) and for  $M_{\infty}$ =0.30~0.80 for the same sweptback wing at k=0.50 are computed by the present 3D NS code, respectively. Results are shown in Fig. 7 for the rectangular wing and in Fig. 8 for the sweptback wing, respectively.

Unfortunately however, no experimental data to be compared with those numerical results is available at this moment. As seen in Figs. 7 and 8, the effect of compressibility on the rolling moment is very small up to  $M_{\infty}$ =0.60. However, some appreciable effect can be seen for Mach number range from 0.70~0.80, where the shock wave appears on the upper surface of the wing. Figures 9 and 10 show the flow patterns (isodensity contours around several span-wise sections and the enlarged 2D flow patterns around the 74% semi-span section of the right wing) during half cycle of oscillation for the rectangular wing at  $M_{\infty}$ =0.75 and k=0.50, and those for the sweptback wing at  $M_{\infty}$ =0.75 and k=0.50, respectively. The flow patterns in Figs.

9 and 10 clearly show the appearance of shock wave and its forward movement accompanied by the shock-induced flow separation during the up-stream movement phases of the right wing, respectively.

# 4 Concluding Remarks

- A numerical simulation method for computing subsonic and transonic flow around a wing oscillating in yaw and sideslip is presented.
- 2) It is demonstrated that the conventional 3D NS code can be modified easily by introducing the new coordinate system fixed on the wing oscillating in yaw and sideslip.
- 3) The computed rolling moments acting on the rectangular and sweptback wings oscillating in yaw show a good agreement with the experimental data in incompressible flow case.
- 4) The capability of the present method for computing the unsteady transonic flow including shock-induced flow separation is demonstrated.
- 5) The present method can easily be extended to T-tail configurations and might present a powerful tool for predicting the effect of compressibility on the flutter speed of T-tail including the effect of the steady load on the horizontal tail plane.

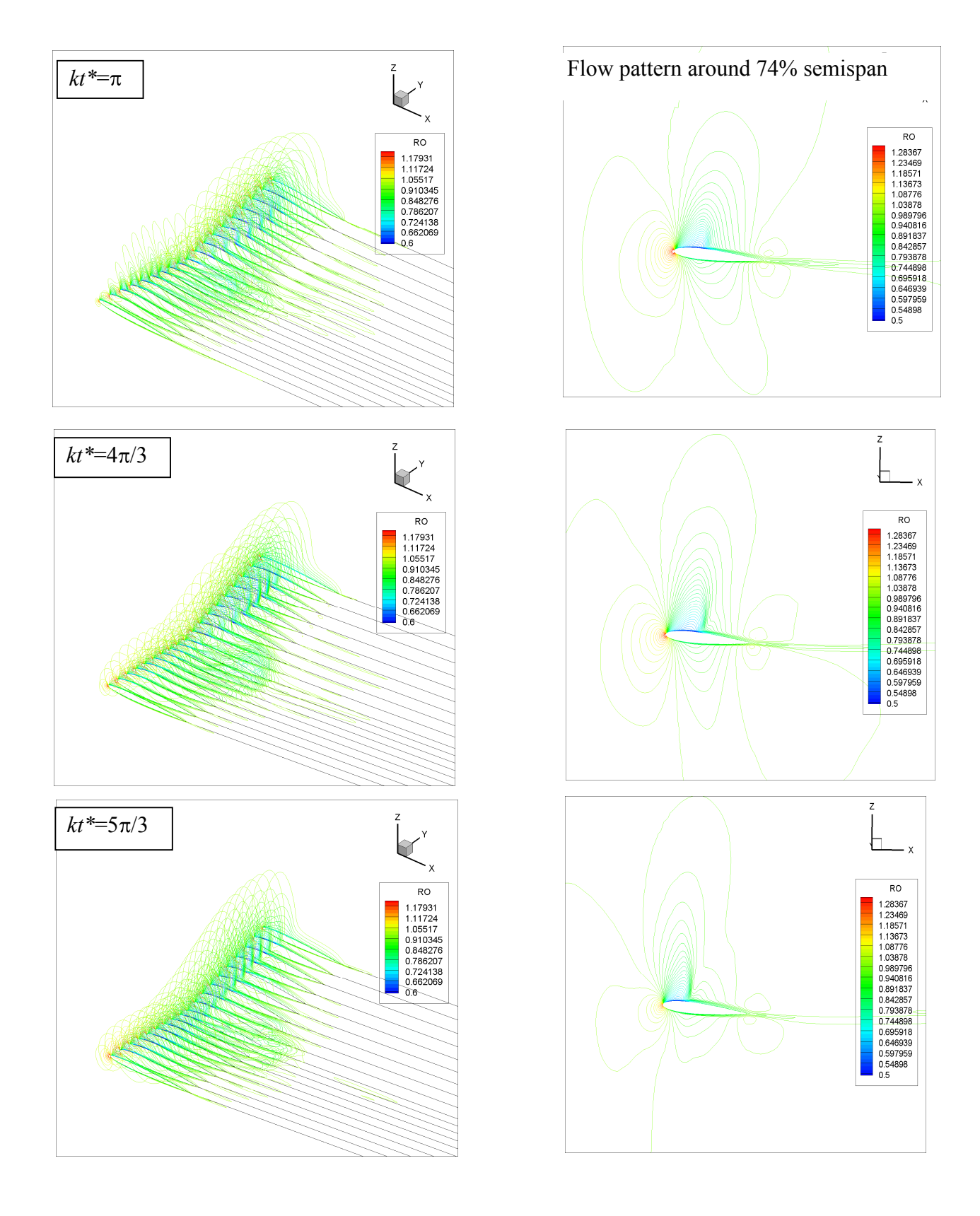


Fig. 9. Flow Patterns (Iso-Density Contours) during Half Cycle of Oscillation (Rectangular Wing,  $M_{\infty}$ =0.75, k=0.50,  $\alpha$ =5.58 deg,  $\Gamma$ =10 deg,  $\Psi$ =6 $^{\circ}$ sinkt\*).

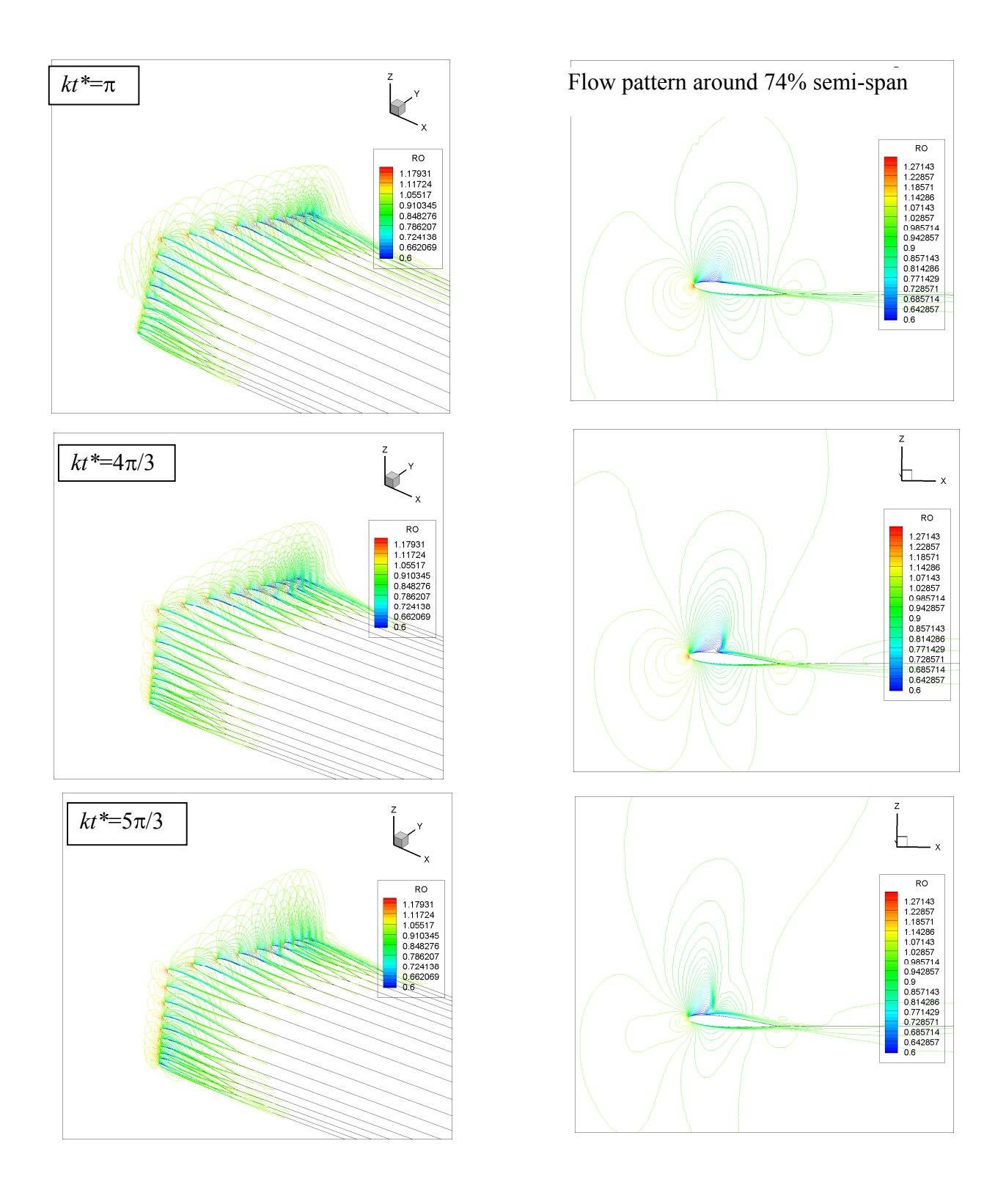


Fig. 10. Flow Patterns (Iso-Density Contours) during Half Cycle of Oscillation (Sweptback Wing,  $M_{\infty}$ =0.75, k=0.50,  $\alpha$ =5.2 deg,  $\Gamma$ =0 deg,  $\Psi$ =6°sinkt\*).

# SUBSONIC AND TRANSONIC FLOW SIMULATION FOR A WING OSCILLATING IN YAW AND SIDE-SLIP

### References

- [1] Baldock J C A. The determination of the flutter speed of a T-tail unit by calculations, model tests and flight flutter tests. *AGARD* Report 221, 1958.
- [2] Washizu K Ichikawa T and Adachi T. A note on T-tail flutter. *Journal of the Japan Society for Aeronautical and Space Sciences*, Vol. 18, No. 200, pp 329-333, 1970. (Japanese Text)
- [3] Jennings W P and Berry M A. Effect of stabilizer dihedral and static lift on T-tail flutter. *Journal of Aircraft*, Vol. 14, No. 4, pp 364-367, 1977.
- [4] Van Zyl L W and Mathews E H. Aeroelastic analysis of T-tails using an enhanced doublet lattice method. *Journal of Aircraft*, Vol. 48, No. 3, pp 823-831, 2011.
- [5] Queijo M J. Theory for computing span loads and stability derivatives due to sideslip, yawing, and rolling for wings in subsonic compressible flow. *NASA* TN D-4929, 1968.
- [6] Isogai K and Ichikawa T. Lifting-surface theory for a wing oscillating in yaw and sideslip with an angle of attack. AIAA Journal, Vol. 11, No. 5, pp 599-606, 1973.
- [7] Isogai K. Lifting-surface theory for an oscillating T-tail, *AIAA Journal*, Vol. 12, No. 1, pp 28-37, 1974.
- [8] Ruhlin C L and Sandford M C. Experimental parametric studies of transonic T-tail flutter. NASA TN D-8066, 1975.
- [9] Arizono H Kheirandish H R and Nakamichi J. Flutter simulation of a T-tail configuration using non-linear aerodynamics. *International Journal for Numerical Methods in Engineering*, 72: 13, pp 1513-1523, 2007.
- [10] Attorni A Cavagna L and Quaranta G. Aircraft T-tail flutter predictions using computational fluid dynamics. *Journal of Fluids and Structures*, 27, pp 161-174, 2011.
- [11] Pulliam T H and Steger J L. Implicit finite-difference simulations of three-dimensional compressible flow. *AIAA Journal*, Vol. 18, No. 2, pp159-167, 1980.
- [12] Isogai K. Numerical simulation of unsteady viscous flow around a flapping wing. *Computational Fluid Dynamics 2002*, edited by Armfield S, et al. Springer, Australia, pp 701-706, 2002.
- [13] Yee H C and Harten A. Implicit TVD schemes for hyperbolic conservation laws in curvilinear coordinates. *AIAA Journal*, Vol. 25, No. 2, pp 266-274, 1987.
- [14] Baldwin B S and Lomax H. Thin layer approximation and algebraic model for separated turbulence flows. *AIAA* Paper 76-267, 1978.
- [15] Ichikawa T Isogai, K Ando Y and Ejiri H. Measurements of rolling moments acting on the stabilizer of T-tails oscillating in yaw. *NAL* TR-324, 1973. (Japanese text)

### **Contact Author Email Address**

Mailto: koji.isogai@nifty.com

## **Copyright Statement**

The authors confirm that they, and/or their company or organization, hold copyright on all of the original material included in this paper. The authors also confirm that they have obtained permission, from the copyright holder of any third party material included in this paper, to publish it as part of their paper. The authors confirm that they give permission, or have obtained permission from the copyright holder of this paper, for the publication and distribution of this paper as part of the ICAS2014 proceedings or as individual off-prints from the proceedings.